



## Changes of medium-range structure in the course of crystallization of zeolite omega from magadiite



Miao Cui<sup>a</sup>, Yifu Zhang<sup>a</sup>, Xiaoyu Liu<sup>a</sup>, Lin Wang<sup>b</sup>, Changgong Meng<sup>a,\*</sup>

<sup>a</sup> School of Chemistry, Dalian University of Technology, Dalian 116024, China

<sup>b</sup> PANalytical, Shanghai 200233, China

### ARTICLE INFO

#### Article history:

Received 29 May 2014

Received in revised form 12 August 2014

Accepted 13 August 2014

Available online 23 August 2014

#### Keywords:

Magadiite

Zeolite omega

Conversion

Medium-range structure

### ABSTRACT

Changes of medium-range structure during the crystallization of zeolite omega from magadiite were characterized. It is found that although the long-range order of magadiite is collapsed in the initial stage, parts of 5-member rings and 6-member rings are still preserved as secondary building units. The fraction of 5-member rings and 6-member rings increases as the crystallization progresses. The 4-member ring chains are formed at a stage later than that of 5-member rings and 6-member rings.

© 2014 Elsevier Inc. All rights reserved.

### 1. Introduction

Zeolites are crystalline aluminosilicates in which the aluminum and silicon atoms are present in the form of  $\text{AlO}_4$  and  $\text{SiO}_4$  tetrahedra. Zeolites have been widely applied to ion exchange, adsorption, catalysis and so on because of their unique structures and properties [1]. Understanding the crystallization mechanisms of zeolites can conduct to exploit efficient routes to synthesize them. Although numerous works have attempted to understand the mechanisms of zeolites and solution transport and solid phase transformation mechanisms are proposed [2–18], relatively few studies have been performed on the elucidation of the medium-range structures and their changes during zeolite crystallization. As it is reported in the previous study, the short-range order is represented by the local coordination polyhedra, while the medium-range structure can be regarded as the next highest level of structural organization beyond the short-range order [19].

Raman spectroscopy is well-known as one of the useful techniques to identify the medium-range structures of zeolites. Xiong et al. have proposed a model of zeolite X formation, which involves 4-membered rings (4Rs) connecting to each other via 6-membered rings (6Rs) to form sod cages, then the sod cages interconnect via double 6-membered rings (D6Rs) to form the FAU-type framework [20]. Dutta et al. proposed the formation mechanisms of zeolite Y and mordenite. It was found that during the crystallization of

zeolite Y, 6Rs interconnect via 4Rs to form sod cages, then the sod cages interconnect via D6Rs to form the FAU-type framework [21]. In the case of mordenite, 4Rs are observed at the early stage followed by a “mordenite-like” amorphous phase with disordered 4Rs and 5-membered rings (5Rs), which then quickly connect to form mordenite crystals [7]. Dutta et al. have also used Raman spectroscopy to study the formation mechanisms of zeolite A [22], ZSM-5 [23] and ferrierite [24].

Atomic pair distribution function (PDF) technique is another powerful method to determine the short and medium-range structures of both disordered and crystallographic materials [25–50]. Recently, this technique has been applied to study the formation mechanisms of zeolites. Wakihara et al. proposed that the formation of faujasite is achieved through sod cages interconnecting with each other via D6Rs [30]. Suzuki et al. observed the changes in medium-range structure during the crystallization of VPI-7, a zirconosilicate zeolite containing 3-membered rings (3Rs). They proposed that the formation of 3Rs is a key process in the crystallization [36]. The formation mechanism of \*BEA-type zeolite was proposed by Inagaki et al. They proposed that double 3-membered rings (D3Rs) contained in the silicate solution transform into “4–2”-type secondary building units (SBUs) in the initial stage. The “4–2”-type SBUs then rearrange to form \*BEA-type framework [49,50].

Synthesizing zeolites by conversion of magadiite, a cheap layered silicate with special structure, is considered to be one commercialization way [51–56]. Comparing to conventional silica source, faster crystallization rate can be obtained by use of magadiite

\* Corresponding author. Tel./fax: +86 411 84708545.

E-mail address: [cgmeng@dlut.edu.cn](mailto:cgmeng@dlut.edu.cn) (C. Meng).

as raw material and the amount of structure directing agent can be decreased for some cases [52]. In our previous work, zeolite omega was synthesized from magadiite in a glycerol–water system [57]. Zeolite omega consists of gmelinite cages which are linked in columns parallel to the *c*-axis to produce main channels with 12-membered rings [58]. In the present work, the elucidation of medium-range structures and their changes during conversion were investigated.

## 2. Experimental

### 2.1. Preparation of magadiite

In this study, magadiite was prepared from colloidal silica (30% SiO<sub>2</sub>). The molar composition of the resultant mixture was SiO<sub>2</sub>:0.15 Na<sub>2</sub>O:4.22 H<sub>2</sub>O. Hydrothermal treatment was carried out at 150 °C for 48 h. After crystallization, the solid products were separated from the mixtures by vacuum filtration and washed with deionized water to pH = 7–8. The products were then dried at 100 °C overnight.

### 2.2. Conversion of magadiite into zeolite omega

The synthetic process was given in detail in previous work of our group [57]. The resultant synthetic solution had the chemical composition of 14 SiO<sub>2</sub>:Al<sub>2</sub>O<sub>3</sub>:10 Na<sub>2</sub>O:169 H<sub>2</sub>O:200 glycerol. Crystallization was carried out under autogenous pressure at 120 °C for 1–10 days. On reaching the crystallization time, a stainless-steel autoclave was taken out of the oven and cooled by water. The solid products were washed with deionized water till pH = 7–8 and dried at 80 °C overnight.

### 2.3. Characterization

The products were identified by a Panalytical X'Pert powder diffractometer at 40 kV and 40 mA with Ni-filtered Cu K $\alpha$  source.

Scanning electron micrograph (SEM) images were obtained with a QUANTA450 scanning electron microscopy.

The Raman spectra were obtained using a Thermo Scientific spectrometer, with a 532 nm excitation line. The Infrared (IR) spectra were measured by a Nicolet 6700 FTIR spectrometer at 2 cm<sup>-1</sup> resolution. Raman and IR spectra were all normalized.

Solid-state <sup>29</sup>Si magic angle spinning nuclear magnetic resonance (MAS NMR) experiments were performed on a Bruker AVANCE III 600 spectrometer at a resonance frequency of 119.2 MHz. <sup>29</sup>Si MAS NMR spectra with high-power proton decoupling were recorded on a 4 mm probe with a spinning rate of 12 kHz, a  $\pi/4$  pulse length of 2.6  $\mu$ s, and a recycle delay of 120 s. The chemical shifts of <sup>29</sup>Si are referenced to TMS.

High-energy X-ray diffraction (HEXRD) experiments were carried out on a Panalytical Empyrean powder diffractometer using Ag K $\alpha$  ( $\lambda = 0.55941$  Å) and a scintillation detector, with incident photon energy of 22 keV. The data were collected from 1.5° to 120° (2 $\theta$ ) with a step length of 0.02 (2 $\theta$ ). The collected data were subjected to well established analysis procedures including absorption, background and the Compton scattering corrections followed by normalization to the total scattering factor,  $S(Q)$ , which is related to the coherent part of the diffraction pattern,  $I^{\text{coh}}(Q)$ , as Eq. (1):

$$S(Q) = 1 + \left[ \frac{I^{\text{coh}}(Q) - \sum c_i |f_i(Q)|^2}{\sum c_i f_i(Q)} \right]^2 \quad (1)$$

where  $I^{\text{coh}}(Q)$  is the measured coherent scattering intensity, and  $c_i$  and  $f_i(Q)$  are the atomic concentration and X-ray atomic form factor, respectively, for atomic species of type *i*. [33] PDF,  $G(r)$ , is derived from Eq. (2),

$$G(r) = \frac{2}{\pi} \int_{Q_{\min}}^{Q_{\max}} Q[S(Q) - 1] \sin(Qr) dQ \quad (2)$$

here,  $Q$  is the magnitude of the wave vector ( $Q = 4\pi \sin \theta / \lambda$ , where  $2\theta$  is the angle between the incoming and outgoing radiation and  $\lambda$  is the wavelength of the incident X-ray radiation).  $Q_{\max}$  collected in this study is 19.4 Å<sup>-1</sup>. In this study, the conversions of the HEXRD data to the PDFs were performed using the program PDF get X2 [59]. Total correlation function,  $T(r)$ , is derived from Eq. (3),

$$T(r) = 4\pi\rho r + \frac{2}{\pi} \int_{Q_{\min}}^{Q_{\max}} Q[S(Q) - 1] \sin(Qr) dQ = 4\pi\rho r + G(r) \quad (3)$$

where  $\rho$  is the total number density [30].

## 3. Results and discussion

### 3.1. Structure of magadiite

The exact structure of magadiite has not been established yet because the small dimensions of single crystals of natural and synthetic magadiite preclude the use of single-crystal X-ray diffraction. Hence, spectroscopic techniques have been used for trying to obtain detailed structural information of magadiite. It has been proposed that magadiite has multilayer structures with 5Rs and 6Rs [60,61]. Fig. 1 shows the IR and Raman spectra of magadiite. The peaks at ca. 1237 and 618 cm<sup>-1</sup> in the IR spectrum are assigned to the existing 5Rs [61] and 6Rs [62] in magadiite, respectively. The Raman spectrum of magadiite gave a major Raman peak at round 465 cm<sup>-1</sup>, which is consistent with that proposed by Huang et al. [60].

### 3.2. Changes of medium-range structure during the crystallization

Fig. 2 shows the X-ray diffraction (XRD) patterns for the magadiite and the products crystallized for 5 days, 6 days, 7 days and 10 days. As the reaction time was increased to 5 days, almost all traces of the magadiite diffraction peaks disappeared as shown in Fig. 2(O 5), indicating the long-range order of magadiite was collapsed after 5 days of heating. When the reaction time was prolonged to 7 days as shown in Fig. 2(O 7), diffraction peaks attributed to zeolite omega appeared. Fig. 2(O 10) shows that pure zeolite omega was obtained after 10 days of crystallization.

Fig. 3 shows solid-state <sup>29</sup>Si MAS NMR spectra for the products crystallized for 5 days, 6 days, 7 days and 10 days. The peaks at ca. 87, 100 and 110 ppm are typical for Q<sup>2</sup>, Q<sup>3</sup> and Q<sup>4</sup>,

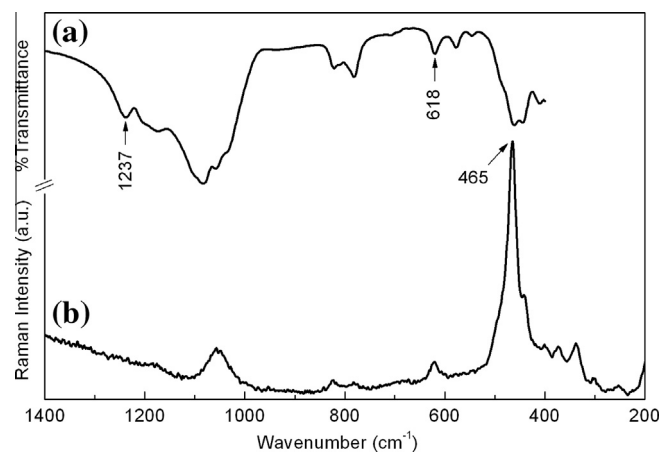


Fig. 1. IR (a) and Raman (b) spectra of magadiite.

Download English Version:

<https://daneshyari.com/en/article/72689>

Download Persian Version:

<https://daneshyari.com/article/72689>

[Daneshyari.com](https://daneshyari.com)